Camera Calibration from the Quasi-affine Invariance of Two Parallel Circles

Yihong Wu, Haijiang Zhu, Zhanyi Hu, and Fuchao Wu

National Laboratory of Pattern Recognition, Institute of Automation, Chinese Academy of Sciences, P.O. Box 2728, Beijing 100080, P.R. China
{yhwu,hjzhu,huzy,fcwu}@nlpr.ia.ac.cn

Abstract. In this paper, a new camera calibration algorithm is proposed, which is from the quasi-affine invariance of two parallel circles. Two parallel circles here mean two circles in one plane, or in two parallel planes. They are quite common in our life.

Between two parallel circles and their images under a perspective projection, we set up a quasi-affine invariance. Especially, if their images under a perspective projection are separate, we find out an interesting distribution of the images and the virtual intersections of the images, and prove that it is a quasi-affine invariance.

The quasi-affine invariance is very useful which is applied to identify the images of circular points. After the images of the circular points are identified, linear equations on the intrinsic parameters are established, from which a camera calibration algorithm is proposed. We perform both simulated and real experiments to verify it. The results validate this method and show its accuracy and robustness. Compared with the methods in the past literatures, the advantages of this calibration method are: it is from parallel circles with minimal number; it is simple by virtue of the proposed quasi-affine invariance; it does not need any matching.

Excepting its application on camera calibration, the proposed quasi-affine invariance can also be used to remove the ambiguity of recovering the geometry of single axis motions by conic fitting method in [8] and [9]. In the two literatures, three conics are needed to remove the ambiguity of their method. While, two conics are enough to remove it if the two conics are separate and the quasi-affine invariance proposed by us is taken into account.

1 Introduction

Camera calibration is an important task in computer vision whose aim is to estimate the camera parameters. Usually, camera self-calibration techniques without prior knowledge on camera parameters are nonlinear [4], [13], [15]. It can be linearized if some scene information is taken into account during the process of calibration. Therefore, it has been appearing a lot of calibration methods using scene constraints [2], [3], [5], [10], [11], [12], [14], [18], [19], [20], [23], [24], [25]. Usually, the used information in the scene is parallels, orthogonality, or

T. Pajdla and J. Matas (Eds.): ECCV 2004, LNCS 3021, pp. 190–202, 2004.

the known angles, circles and their centers, concentric conics et al. For example, in [14], the images of circular points are determined when there is a circle with several diameters in the scene, then the linear constraints on the intrinsic parameters are set up. In [2], by using the parallel and orthogonal properties of the scene, the constraints on the projective matrix are given. Parallelepipeds with some known angles and length ratios of the sides are assumed existed, then from them the equations on the intrinsic parameters are established in [20]. [25] presents a calibration method using one-dimensional objects.

Our idea in this paper is also to use the scene information to find the constraints on the intrinsic parameters of cameras. Two circles in one plane or in two parallel planes, called two parallel circles, are assumed to be in the scene, and then a quasi-affine invariance of them is found. Based on the invariance, camera calibration is investigated, and a new algorithm is proposed. Compared with the previous methods, this method has the following advantages: it is from parallel circles with minimal number; it is simple by virtue of the proposed quasi-affine invariance; it does not need any matching.

The parallel circles are quite common in our life, and then this calibration method can be applied. It can also be used to solve the ambiguity for recovering the geometry of single axis motions in [8], [9]. The two literatures have shown that the geometry of single axis motion can be recovered given at least two conic loci consisting of corresponding image points over multiple views. If the two conics are separate or enclosing, the recovery has a two fold ambiguity, the ambiguity is removed by using three conics in the literatures. In fact, if the two conics are separate, it is enough to remove the ambiguity only from the two conics by taking into account the quasi-affine invariance presented in this paper.

On the other hand, in [16], Quan gave the invariants of two space conics. When the two conics are parallel circles, this invariants cannot be set up, but a quasi-affine invariance proposed in this paper indeed exists. Actually, the imaging process of a pinhole camera is quasi-affine [6], [7], the proposed quasi-affine invariance is very useful.

The paper is organized as follows. Section 2 is some preliminaries. Section 3 uses a quasi-affine invariance of two parallel circles to establish the equations on the camera intrinsic parameters, and gives a linear algorithm for calibrating a camera from these equations. Then, the invariance and algorithm are validated from both simulated and real experiments in Section 4. Conclusions and acknowledgements are remarked in Section 5 and 6 respectively.

2 Preliminaries

In this paper, "$\approx$" denotes the equality up to a scale, a capital bold letter denotes a matrix or a 3D homogeneous coordinates, a small bold letter denotes a 2D homogeneous coordinates.

Definition 1. *If two circles in space are in one plane, or in two parallel planes respectively, we call them two parallel circles.*

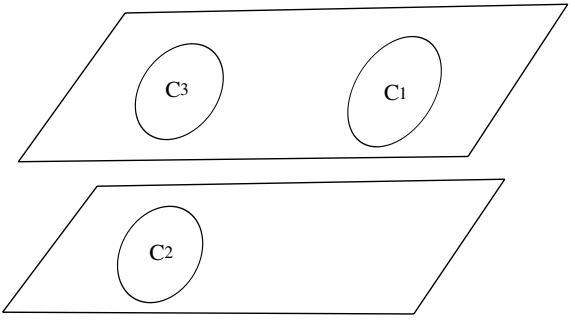

Fig. 1. Parallel circles. $\mathbf{C}_1$ and $\mathbf{C}_3$ are coplanar, $\mathbf{C}_2$ is in the plane parallel to the plane containing $\mathbf{C}_1$ and $\mathbf{C}_3$. Any two of them are two parallel circles

See Fig. 1, $\mathbf{C}_1$, $\mathbf{C}_2$, $\mathbf{C}_3$ are parallel circles each other.

Under a pinhole camera, a point $\mathbf{X}$ in space is projected to a point $\mathbf{x}$ in the image by:

$$\mathbf{x} \approx \mathbf{K}[\mathbf{R}, \mathbf{t}]\mathbf{X}, \tag{1}$$

where $\mathbf{K}$ is the 3×3 matrix of camera intrinsic parameters, $\mathbf{R}$ is a 3×3 rotation matrix, $\mathbf{t}$ is a 3D translation vector. The goal of calibrating a camera is to find $\mathbf{K}$ from images.

The absolute conic consists of points $\mathbf{X} = (X_1, X_2, X_3, 0)$ at infinity such that:

$$X_1^2 + X_2^2 + X_3^2 = 0, \quad \text{or,} \quad \mathbf{X}^\tau \mathbf{X} = 0,$$

and its image ω is:

$$\mathbf{x}^\tau \mathbf{K}^{-\tau} \mathbf{K}^{-1} \mathbf{x} = 0. \tag{2}$$

If some points on ω can be inferred from image, the equations on the intrinsic parameters can be set up by (2). If the number of these equations is enough, the intrinsic parameters will be determined. In the following, we are to find the points on ω by using two parallel circles in the scene.

Some preliminaries on projective geometry are needed, the readers can refer to the details in [17]. Every real plane other than the plane at infinity, denoted by P, intersects the plane at infinity at a real line, called the line at infinity of P, denoted by L_0. L_0 intersects the absolute conic at a pair of conjugate complex points, called the circular points of P. Every circle in P passes through the circular points of P. Let $\mathbf{C}_1$ and $\mathbf{C}_2$ be two parallel circles, P_1 and P_2 be the parallel planes containing them. Because P_1 and P_2 have the same line at infinity, they have the same pair of circular points. Therefore, $\mathbf{C}_1$ and $\mathbf{C}_2$ pass through the same pair of circular points, they and the absolute conic form a coaxial conic system at the two circular points (A coaxial conic system means a set of conics through two fixed points).

A quasi-affine transformation lies part way between a projective and affine transformation, which preserves the convex hull of a set of points, and the relative

positions of some points and lines in a plane, or the relative positions of some points and planes in 3D space. For the details, see [7] or Chapter 20 in [6].

3 New Calibration Method from the Quasi-affine Invariance of Two Parallel Circles

Under a pinhole camera, a circle is projected to a conic. Moreover, because **K, R, t** in (1) are real, a real point is projected to a real point, and a pair of conjugate complex is projected to a pair of conjugate complex. So the images of a pair of circular points must still be a pair of conjugate complex.

If there are three or more than three parallel circles in the scene, then from their images, the images of a pair of circular points can be uniquely determined without any ambiguity by solving for the intersection points of the three image conics [8], [21]. If there are only two ones in the scene, denoted by $\mathbf{C}_1$, $\mathbf{C}_2$, whose images are denoted by $\mathbf{c}_1$, $\mathbf{c}_2$, whether the images of a pair of circular points can be uniquely determined or not depends on the relative positions of $\mathbf{c}_1$ and $\mathbf{c}_2$. The equations for $\mathbf{c}_1$, $\mathbf{c}_2$ are two quadric equations, the number of their common solutions over complex field is four with multiplicity. If there are real solutions among these four ones, or $\mathbf{c}_1$ and $\mathbf{c}_2$ have real intersections, then there is a unique pair of conjugate complex among these four solutions, which must be the images of the pair of circular points. If $\mathbf{c}_1$ and $\mathbf{c}_2$ have no real intersection, these four solutions are two pairs of conjugate complex. Which pair is the images of the circular points? We will discuss it in the following.

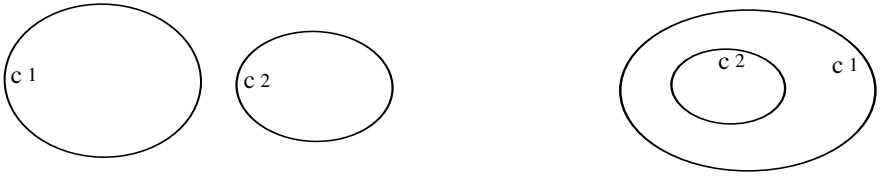

Fig. 2. Two cases that $\mathbf{c}_1$ and $\mathbf{c}_2$ have no real intersection: the left side is the separate case; the right side is the enclosing case

If the relative positions of the camera and circles in the scene are in general, or, the circles lie entirely in front of the camera, the images of these circles are ellipses. From now, we always regard that the circles in the scene are entirely in front of the camera. Then, when $\mathbf{c}_1$ and $\mathbf{c}_2$ have no real intersection, there are two cases as shown in Fig. 2, one case is that $\mathbf{c}_1$ and $\mathbf{c}_2$ separate; another case is that $\mathbf{c}_1$ and $\mathbf{c}_2$ enclose. For the enclosing case, we can not distinguish the images of the circular points between the two pairs of conjugate complex intersections of $\mathbf{c}_1$ and $\mathbf{c}_2$ [21]. While, for the separate case, we can distinguish them by a quasi-affine invariance.

Firstly, a lemma with respect to two coplanar circles is needed. In order to distinguish notations of two coplanar circles from the above notations $\mathbf{C}_1$ and $\mathbf{C}_2$ of two parallel circles, we denote two coplanar circles as $\mathbf{C}_1$ and $\mathbf{C}_3$.

Lemma 1. *If* $\mathbf{C}_1$ *and* $\mathbf{C}_3$ *are two coplanar separate circles, their homogeneous equations have two pairs of conjugate complex common solutions. We connect the two points in each pair of the conjugate complex common solutions, then obtain two real lines, called the associated lines of* $\mathbf{C}_1$ *and* $\mathbf{C}_3$*. One of the two associated lines lies between* $\mathbf{C}_1$ *and* $\mathbf{C}_3$*, and the other one, which is the line at infinity passing through the circular points, does not lie between* $\mathbf{C}_1$ *and* $\mathbf{C}_3$ *as shown in Fig. 3.*

The proof of Lemma 1 is given in Appendix.

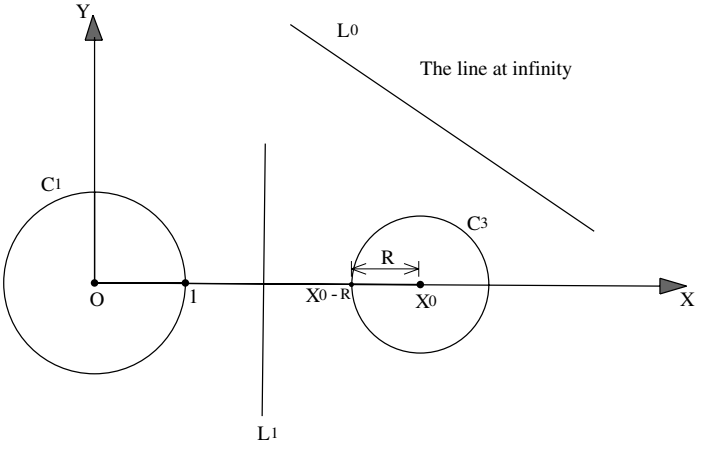

Fig. 3. Two coplanar separate circles $\mathbf{C}_1$, $\mathbf{C}_3$, and their associated lines $\mathbf{L}_1$ and $\mathbf{L}_0$ (the line at infinity). $\mathbf{C}_1$ and $\mathbf{C}_3$ intersect at two pairs of conjugate complex points, one pair is on the line $\mathbf{L}_1$; another pair, which is the pair of circular points, is on the line at infinity $\mathbf{L}_0$. $\mathbf{L}_1$ lies between $\mathbf{C}_1$ and $\mathbf{C}_3$, while, $\mathbf{L}_0$ does not

Theorem 1. *If* $\mathbf{c}_1$*,* $\mathbf{c}_2$ *are the images of two parallel circles and separate, their homogeneous equations have two pairs of conjugate complex common solutions. We connect the two points in each pair of the conjugate complex common solutions, then obtain two real lines, called the associated lines of* $\mathbf{c}_1$ *and* $\mathbf{c}_2$*. One of the two associated lines lies between* $\mathbf{c}_1$ *and* $\mathbf{c}_2$*, and the other one does not lie between* $\mathbf{c}_1$ *and* $\mathbf{c}_2$ *as shown in Fig. 4. If the camera optical center does not lie between the two parallel planes containing the two circles, the associated line not lying between* $\mathbf{c}_1$ *and* $\mathbf{c}_2$ *is the vanishing line through the images of circular points. Otherwise, the associated line lying between* $\mathbf{c}_1$ *and* $\mathbf{c}_2$ *is the vanishing line through the images of circular points.*

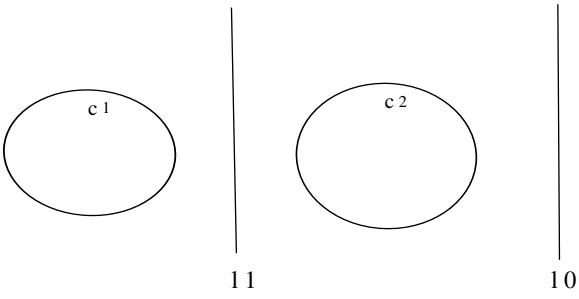

Fig. 4. The distributions of $\mathbf{c}_1$, $\mathbf{c}_2$, and their two associated lines $\mathbf{l}_1$ and $\mathbf{l}_0$. $\mathbf{c}_1$ and $\mathbf{c}_2$ intersect at two pairs of conjugate complex points, one pair is on the line $\mathbf{l}_1$; another pair is on the line $\mathbf{l}_0$. $\mathbf{l}_1$ lies between $\mathbf{c}_1$ and $\mathbf{c}_2$, while, $\mathbf{l}_0$ does not. The images of circular points are the pair on $\mathbf{l}_0$ if the optical center does not lie between the two parallel planes containing the two circles. Otherwise, they are the pair on $\mathbf{l}_1$

Proof. Let the two parallel circles be $\mathbf{C}_1$, $\mathbf{C}_2$, and P_1, P_2 be the planes containing them, $\mathbf{O}$ be the camera optical center. Because P_1, P_2 are parallel, the quadric cone with $\mathbf{O}$ as its vertex and passing through $\mathbf{C}_2$ intersects the plane P_1 at a circle, denoted by $\mathbf{C}_3$. $\mathbf{C}_1$ and $\mathbf{C}_3$ are two coplanar circles in P_1. Because $\mathbf{c}_1$ and $\mathbf{c}_2$ are separate, and are also the images of $\mathbf{C}_1$ and $\mathbf{C}_3$, we know that $\mathbf{C}_1$ and $\mathbf{C}_3$ are separate too. See Fig. 5. By Lemma 1, there is the fact: one of the associated lines of $\mathbf{C}_1$ and $\mathbf{C}_3$ lies between $\mathbf{C}_1$ and $\mathbf{C}_3$ (denoted by L), and the other one, i.e. the line at infinity passing through the circular points, does not lie between $\mathbf{C}_1$ and $\mathbf{C}_3$ (denoted by L_0).

If $\mathbf{O}$ does not lie between P_1 and P_2, we know that $\mathbf{C}_1$, $\mathbf{C}_3$ in P_1 are all in front of the camera. Because under a pinhole camera, the imaging process from the parts of P_1 in front of the camera to the image plane is quasi-affine ([7], Chapter 20 in [6]), the relative positions of $\mathbf{c}_1$, $\mathbf{c}_2$ and their associated lines are the same as the ones of $\mathbf{C}_1$, $\mathbf{C}_3$, L, L_0. So the associated line not lying between $\mathbf{c}_1$ and $\mathbf{c}_2$ is the images of L_0, i.e. the vanishing line through the images of the circular points.

If $\mathbf{O}$ lies between P_1 and P_2, the plane through $\mathbf{O}$ and L_0, denoted by P_0, which is parallel to P_1 and P_2, lies between $\mathbf{C}_1$ and $\mathbf{C}_2$. And, the plane through $\mathbf{O}$ and L, denoted by P, does not lie between $\mathbf{C}_1$ and $\mathbf{C}_2$. This is because $\mathbf{C}_3$ and $\mathbf{C}_1$ lie on the different sides of P, and also $\mathbf{C}_3$ and $\mathbf{C}_2$ lie on the different sides of P. The projection from $\mathbf{C}_1$, $\mathbf{C}_2$, P_0, P to their images is quasi-affine, so $\mathbf{c}_1$, $\mathbf{c}_2$ and their associated lines have the same relative positions as the ones of $\mathbf{C}_1$, $\mathbf{C}_2$, P_0, P (The image of P_0 is the vanishing line lying between $\mathbf{c}_1$ and $\mathbf{c}_2$, the image of P is the associated line not lying between $\mathbf{c}_1$ and $\mathbf{c}_2$).

Then, the theorem is proved.

Therefore, if $\mathbf{c}_1$ and $\mathbf{c}_2$ are separate, by Theorem 1, we can find out the images of a pair of circular points. If $\mathbf{c}_1$ and $\mathbf{c}_2$ are enclosing, and their two pairs of conjugate complex intersections do not coincide, we can not find out the images of circular points now (if the two pairs of conjugate complex intersections

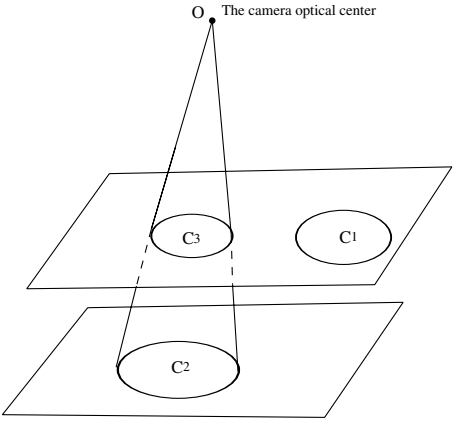

Fig. 5. The camera and two parallel circles $\mathbf{C}_1$, $\mathbf{C}_2$. $\mathbf{O}$ is the camera optical center. The quadric cone passing through $\mathbf{O}$ (as the vertex) and $\mathbf{C}_2$ intersects the plane containing $\mathbf{C}_1$ at another circle $\mathbf{C}_3$. $\mathbf{C}_1$ and $\mathbf{C}_3$ are coplanar. If the images of $\mathbf{C}_1$ and $\mathbf{C}_2$ are separate, $\mathbf{C}_1$ and $\mathbf{C}_3$ are separate too because the image of $\mathbf{C}_3$ is the same as the image of $\mathbf{C}_2$

coincide to one pair, the coinciding pair is the images of circular points, and at the time, $\mathbf{C}_1$, $\mathbf{C}_3$ are concentric) [21].

In fact, the enclosing case of $\mathbf{c}_1$ and $\mathbf{c}_2$ usually seldom occurs, and other cases of $\mathbf{c}_1$ and $\mathbf{c}_2$ occur quite often in our life. We regard that $\mathbf{c}_1$ and $\mathbf{c}_2$ are not enclosing below.

By the discussion in the second paragraph in this section and Theorem 1, the images of a pair of circular points can always be determined from a single view of two parallel circles. Assuming the images of the determined circular points to be $\mathbf{m}_I$, $\mathbf{m}_J$, by (2), we have two linear equations on the camera intrinsic parameters $\omega = \mathbf{K}^{-\tau}\mathbf{K}^{-1}$ as:

$$\mathbf{m}_I^{\tau}\omega\ \mathbf{m}_I = 0, \quad \mathbf{m}_J^{\tau}\omega\ \mathbf{m}_J = 0. \tag{3}$$

If the camera intrinsic parameters are kept unchanged and the motions between cameras are not pure translations, then from three views, six linear equations on the intrinsic parameters can be set up. Thus, the camera can be calibrated completely.

An outline of our algorithm to calibrate a camera from the images of two parallel circles is showed as follows.

Step 1. In each view, extract the pixels $\mathbf{u}$ of the images of two parallel circles, and fit them with $\mathbf{u}^{\tau}\mathbf{c}_1\mathbf{u} = 0$, $\mathbf{u}^{\tau}\mathbf{c}_2\mathbf{u} = 0$ to obtain $\mathbf{c}_1$ and $\mathbf{c}_2$ by the least squares method, then establish two conic equations as $e_1 : \mathbf{x}^{\tau}\mathbf{c}_1\mathbf{x} = 0$, and $e_2 : \mathbf{x}^{\tau}\mathbf{c}_2\mathbf{x} = 0$.

Step 2. Solve the common solutions of e_1, e_2 in each view.

Step 3. Find out the images of the circular points from the solved common solutions of e_1, e_2 by the method presented in this section.

Step 4. Set up the equations on the intrinsic parameters $\omega = \mathbf{K}^{-\tau}\mathbf{K}^{-1}$ from the images of circular points found out in Step 3 by (3).

Step 5. Solve out ω from the equations in Step 4 by singular value decomposition method, and then do Cholesky decomposition and inverse the result, or use the equations in [22], to obtain the intrinsic parameters $\mathbf{K}$.

Remark 1. With the notations $\mathbf{O}$, L, L_0 as in the proof of Theorem 1, let P be the plane through $\mathbf{O}$ and L, P_0 be the plane through $\mathbf{O}$ and L_0. By the proof of Theorem 1, we know that the relative positions of $\mathbf{C}_1$, $\mathbf{C}_2$, P, P_0 are the same as the ones of their images, which just is a **quasi-affine invariance**. For other cases except for the enclosing case, the images of circular points are found out by the real projective invariance preserving the real and conjugate complex intersections of conics respectively. Of course, the projective invariance is also a **quasi-affine invariance**.

Remark 2. In Theorem 1, there are two cases: one case is that the optical center does not lie between the two parallel planes P_1, P_2 containing the two circles; another case is that the optical center lies between P_1 and P_2. In general, the former case occurs more often than the latter case. When the two circles are coplanar, the optical center always does not lie between P_1 and P_2, the associated line of $\mathbf{c}_1$ and $\mathbf{c}_2$ not lying between $\mathbf{c}_1$ and $\mathbf{c}_2$ is always the vanishing line.

Remark 3. If we use the above method with a calibration grid to calibrate camera in the same way as Zhang's method [24], it might be wise to take two intersecting coplanar circles.

4 Experiments

4.1 Simulated Experiments

In the experiments, the simulated camera has the following intrinsic parameters:

$$\mathbf{K} = \begin{bmatrix} 1500 & 3 & 512 \\ 0 & 1400 & 384 \\ 0 & 0 & 1 \end{bmatrix}.$$

Take two parallel circles in the world coordinates system as: $X^2 + Y^2 = 6^2, Z = 0$; $(X-20)^2 + Y^2 = 3^2, Z = 10$. And, take three groups of rotation axes, rotation angles and translations as: $\mathbf{r}_1 = (17, 50, 40)^\tau, \theta_1 = 0.3\pi, \mathbf{t}_1 = (-5, 15, 50)^\tau$; $\mathbf{r}_2 = (-50, 50, 160)^\tau, \theta_2 = 0.1\pi, \mathbf{t}_2 = (10, -4, 40)^\tau$; $\mathbf{r}_3 = (90, -70, 20)^\tau, \theta_3 = 0.2\pi, \mathbf{t}_3 = (5, 2, 30)^\tau$. Let $\mathbf{R}_i$ be the rotations from $\mathbf{r}_i$, θ_i. Then project the two circles to the simulated image planes by the three projective matrices $\mathbf{P}_i = \mathbf{K}[\mathbf{R}_i, \mathbf{t}_i], i = 1, 2, 3$ respectively. The images of the two circles are all separate (in order to verify Theorem 1), and the image sizes are of 700×900, 550×950, 500×850 pixels respectively. Gaussian noise with mean 0 and standard deviation ranging from 0 to 2.0 pixels is added to the image points of the two

Table 1. The averages of the estimated intrinsic parameters under different noise levels

Noise levels(pixel)	f_u	f_v	s	u_0	v_0
0	1500.0000	1400.0000	3.0000	511.9999	384.0000
0.4	1500.4522	1400.4622	3.0655	513.0418	384.7355
0.8	1500.3927	1399.8069	2.6278	518.8032	389.0022
1.2	1500.9347	1399.9088	2.8893	525.2412	392.4559
1.6	1501.8536	1399.4255	3.2259	537.6676	399.6847
2.0	1503.9747	1399.7978	2.4428	548.5837	410.4403

Table 2. The RMS errors of the estimated intrinsic parameters under different noise levels

Noise levels(pixel)	f_u	f_v	s	u_0	v_0
0	0.0000	0.0000	0.0000	0.0000	0.0000
0.4	5.1775	4.7679	0.8985	5.1834	5.2046
0.8	11.1786	10.2244	1.8713	11.2057	11.2147
1.2	15.6606	14.3364	2.7034	15.6643	15.9711
1.6	21.1434	19.9497	3.0504	21.4699	21.1630
2.0	26.6784	24.8587	4.8918	27.6128	27.0722

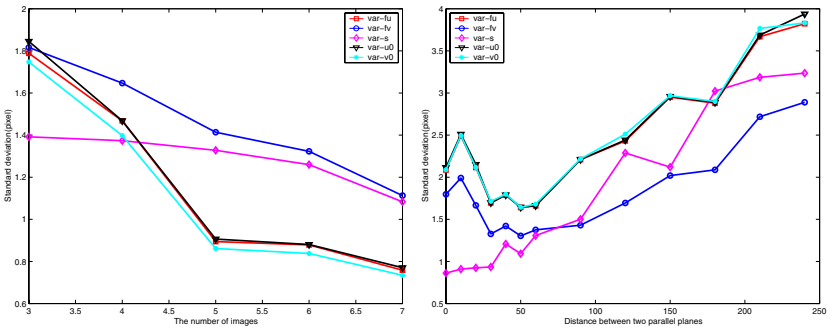

(a) (b)

Fig. 6. The standard deviations of the estimated intrinsic parameters vs. (a) the number of images; (b) the distance of the two parallel circles (defined to be the distance of the two parallel planes containing the two circles)

circles, and then the intrinsic parameters are computed. For each noise level, we perform 50 times independent experiments, and the averaged results are shown in Table 1. We also compute the root mean square errors (RMS errors) of intrinsic parameters under different noise levels, the results are given in Table 2.

In order to assess the performance of our calibration technique with the number of images and with the distance of the two parallel circles, the calibrations using 4, 5, 6, 7 images and varying the distance of the two circles are performed respectively, and the standard deviations of the estimated intrinsic parameters are shown in Fig. 6, where the added noise level is 0.5 pixels. It is clear that the deviations tend to decrease with the number of the images increasing. Let d be the distance of the two parallel planes containing the two circles (the two circles used are: $X^2 + Y^2 = 10^2, Z = 0$ and $(X - 40)^2 + Y^2 = 10^2, Z = d$. d is varying from 0 to 240). Then we can see that: (i) the deviations for f_u, f_v, u_0, v_0 tend to decrease with d increasing from 0 to 50, and then to increase with d increasing from 50 to 240; (ii) the deviations for s tend to increase with d increasing. It follows that it is not the coplanar circles such that the algorithm is most stable.

Fig. 7. The used three images of two parallel circles

4.2 Real Experiments

We use a CCD camera to take three photos of two cups as shown in Fig. 7. The photos are of 1024×768 pixels. In each photo, the pixels of the images of the upper circles at the brim of the two cups are extracted, then fitted by the least squares method to obtain two conic equations (see Step 1 of our algorithm). From Fig. 7, we can see that the extracted conics are separate in each view. Applied Theorem 1 and the proposed calibration algorithm to these conic equations, the estimated intrinsic parameter matrix is:

$$\mathbf{K}_1 = \begin{bmatrix} 1409.3835 & 8.0417 & 568.2194 \\ 0 & 1385.3772 & 349.3042 \\ 0 & 0 & 1 \end{bmatrix}.$$

To verify $\mathbf{K}_1$, the classical calibration grid DLT method in [1] is used to calibrate the same camera (the intrinsic parameters keep unchanged). The used

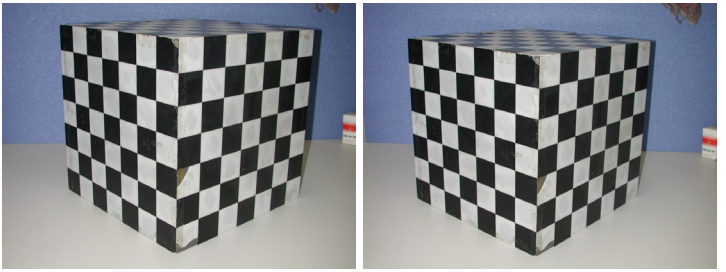

Fig. 8. The used images of a calibration grid

image is the left one in Fig. 8, and the calibration result from 72 corresponding pairs of space and image points is:

$$\mathbf{K}_2 = \begin{bmatrix} 1325.6124 & 4.5399 & 500.7259 \\ 0 & 1321.2270 & 368.4573 \\ 0 & 0 & 1 \end{bmatrix}.$$

The estimated intrinsic parameters $\mathbf{K}_1$, $\mathbf{K}_2$ are used to reconstruct the calibration grid from the two images in Fig. 8. The angles between two reconstructed orthogonal planes are:

$$89.28^\circ \text{ by using } \mathbf{K}_1, \qquad 89.97^\circ \text{ by using } \mathbf{K}_2.$$

Both of them are close to the ground truth of 90°. Consider the reconstructed vertical parallel lines on the calibration grid, then compute the angles between any two of them, and the averages are:

$$0.0000476^\circ \text{ by using } \mathbf{K}_1, \qquad 0.0000395^\circ \text{ by using } \mathbf{K}_2.$$

Both of them are close to the ground truth of 0°. These results validate the proposed algorithm in this paper.

5 Conclusions

We presented a quasi-affine invariance of two parallel circles, then applied it to calibrating a camera. Both simulated and real experiments were given, and showed the accuracy and robustness of this method. The presented quasi-affine invariance is quite interesting and useful. It can also be applied to recovering the geometry of single axis motions by conic fitting method. We believe that it will have more applications in future.

Acknowledgements. We would like to thank the reviewers for their suggestions. The work is supported by the National Key Basic Research and Development Program (973) under grant No. 2002CB312104 and the National Natural Science Foundation of China under grant No. 60121302.

References

1. Y.I. Abdel-Aziz, and H.M. Karara: Direct linear transformation from comparator coordinates into object space coordinates in close-range photogrammetry. *Proc. ASP/UI Symp. on CloseRange Photogrammetry*, pp. 1–18, 1971.
2. D. Bondyfalat, T. Papadopoulo, and B. Mourrain: Using scene constraints during the calibration procedure. *ICCV*, pp. 124–130, 2001.
3. B. Caprile, and V. Torre: Using vanishing points for camera calibration. *International Journal of Computer Vision*, 4(2), 127–140, 1990.
4. O.D. Faugeras, Q.T. Luong, and S. Maybank: Camera self-calibration: theory and experiments. *ECCV*, pp. 321–334, 1992.
5. V. Fremont, and R. Chellali: Direct camera calibration using two concentric circles from a single view. *ICAT*, pp. 93–98, 2002.
6. R. Hartley, and A. Zisserman: *Multiple view geometry in computer vision*. Cambridge University press, 2000.
7. R. Hartley: Chirality. *International Journal of Computer Vision*, 26(1), 41–61, 1998.
8. G. Jiang, H.T. Tsui, L. Quan, and A. Zisserman: Single axis geometry by fitting conics. *ECCV*, LNCS 2350, pp. 537–550, 2002.
9. G. Jiang, H.T. Tsui, L. Quan, and S.Q. Liu: Recovering the geometry of single axis motions by conic fitting. *CVPR*, pp. 293–298, 2001.
10. J-S Kim, H-W Kim, and I.S. Kweon: A camera calibration method using concentric circles for vision applications. *ACCV*, pp. 515–520, 2002.
11. D. Liebowitz, and A. Zisserman: Metric rectification for perspective images of planes. *CVPR*, pp. 482–488, 1998.
12. D. Liebowitz, and A. Zisserman: Combining scene and auto-calibration constraints. *ICCV*, pp. 293–300, 1999.
13. Q.T. Luong, and O.D. Faugeras: Self-calibration of a moving camera from point correspondence and fundamental matrices. *International Journal of Computer Vision*, 22(3), 261–289, 1997.
14. X.Q. Meng, and Z.Y. Hu: A new easy camera calibration technique based on circular points. *Pattern Recognition*, 36(5), 1155–1164, 2003.
15. M. Pollefeys, R. Koch, and L. Van Gool: Self-calibration and metric reconstruction in spite of varying and unknown intrinsic camera parameters. *ICCV*, pp. 90–95, 1998.
16. L. Quan: Invariant of a pair of non-coplanar conics in space: definition, geometric interpretation and computation. *ICCV*, pp. 926–931, 1995.
17. J.G. Semple, and G.T. Kneebone: *Algebraic projective geometry*. Oxford University Press, 1952.
18. P. Sturm, and S. Maybank: On plane-based camera calibration: a general algorithm, singularities, applications. *CVPR*, pp. 432–437, 1999.
19. R.Y. Tsai: A versatile camera calibration technique for accuracy 3D machine vision metrology using off-the-shelf TV cameras and lences. *IEEE Journal of Robotics and Automation*, 3(4), 323–344, 1987.
20. M. Wilczkowiak, E. Boyer, and P. Sturm: Camera calibration and 3D reconstruction from single images using parallelepipeds. *ICCV*, pp. 142–148, 2001.
21. Y.H. Wu, X.J. Li, F.C. Wu, and Z.Y. Hu: Coplanar circles, quasi-affine invariance and calibration. http://www.nlpr.ia.ac.cn/english/rv/∼yhwu/papers.htm, 2002.
22. Y.H. Wu, and Z.Y. Hu: A new constraint on the imaged absolute conic from aspect ratio. http://www.nlpr.ia.ac.cn/english/rv/∼yhwu/papers.htm, 2003.

23. C.J. Yang, F.M. Sun, and Z.Y. Hu: Planar conic based camera calibration. *ICPR*, pp. 555–558, 2000.
24. Z. Zhang: A flexible new technique for camera calibration. *IEEE Transaction on Pattern Analysis and Machine Intelligence*, 22(11), 1330–1334, 2000.
25. Z. Zhang: Camera calibration with one-dimensional objects. *ECCV*, pp. 161–174, 2002.

Appendix: Proof of Lemma 1

$\mathbf{C}_1$, $\mathbf{C}_3$ are coplanar and separate, then we can set up the Euclidean coordinate system as: one of the centers of $\mathbf{C}_1$ and $\mathbf{C}_3$ as the origin $\mathbf{O}$, the line through the two centers as the X-axis, the line through $\mathbf{O}$ and orthogonal to the X-axis as the Y-axis, the radius of one of the circles as the unit length. For example, we take the coordinate system as in Fig. 3. Then the homogeneous equations of $\mathbf{C}_1$ and $\mathbf{C}_3$ are respectively:

$$X^2 + Y^2 = Z^2, \quad (X - X_0 Z)^2 + Y^2 = R^2 Z^2 \tag{4}$$

where R is the radius of $\mathbf{C}_3$, X_0 horizontal coordinate of the center of $\mathbf{C}_3$. Because $\mathbf{C}_1$ and $\mathbf{C}_3$ separate, $X_0 > 1 + R$. Solve the common solutions of (4), and compute the associated lines, then we have them as:

$$\mathbf{L}_1 : X = \frac{X_0^2 - R^2 + 1}{2X_0}, \qquad \mathbf{L}_0 : Z = 0 \ \text{ (the line at infinity)}$$

Because $X_0 > 1 + R$, we can prove that the following inequality holds:

$$1 < \frac{X_0^2 - R^2 + 1}{2X_0} < X_0 - R < \infty$$

From the inequality, we know that $\mathbf{C}_1$, $\mathbf{C}_3$ lie on the different sides of $\mathbf{L}_1$. Since $\mathbf{L}_0$ is at infinity, $\mathbf{C}_1$, $\mathbf{C}_3$ must lie on the same side of it as shown in Fig. 3.

In addition, the above proof is independent of the chosen Euclidean coordinate system. This is because if we set up another Euclidean coordinate system (with the same or different unit length as the above one), they can be transformed each other by a Euclidean transformation, or a similarity transformation, which preserves the line at infinity and preserves the relative positions of objects.